2006

Modeling Volume Changes in Porous Electrodes

Parthasarathy M. Gomadam
University of South Carolina - Columbia

John W. Weidner
University of South Carolina - Columbia, weidner@engr.sc.edu

Publication Info

Journal of the Electrochemical Society, 2006, pages A179-A186.

Publisher's link: http://dx.doi.org/10.1149/1.2136087
DOI:10.1149/1.2136087

Journal of The Electrochemical Society, **153** (1) A179-A186 (2006)
0013-4651/2005/153(1)/A179/8/$20.00 © The Electrochemical Society, Inc.

Modeling Volume Changes in Porous Electrodes

Parthasarathy M. Gomadam*,[a,z] and John W. Weidner**

Center for Electrochemical Engineering, Department of Chemical Engineering, University of South Carolina, Columbia, South Carolina 29208, USA

A three-dimensional mathematical model is presented to describe volume changes in porous electrodes occurring during operation. Material conservation equations are used to derive governing relationships between electrode dimensions and porosity for deposition/precipitation, intercalation, and ionomer-based electrodes. By introducing a parameter, called the swelling coefficient, the relative magnitudes of the change in electrode dimensions and the change in porosity are determined. The swelling coefficient is design-dependent and measured experimentally for a given cell design. The model is general and forms a critical addition required to extend the existing porous electrode models to include volume change effects. For the special case of uniform reaction distribution, analytical solutions are presented and used to illustrate the effect of volume changes in porous electrodes.
 [DOI: 10.1149/1.2136087]

Manuscript submitted July 29, 2005; revised manuscript received September 22, 2005.
Available electronically December 12, 2005.

Many researchers have reported significant volume changes occurring in porous electrodes. For example, in Li–$SOCl_2$ batteries precipitation of LiCl causes significant cathode swelling and is considered an important phenomenon governing the evolution of cell resistance during discharge.[1] In Li-ion batteries, volume changes as high as 358% have been observed by Yang et al.[2] with Li–Sn alloy intercalation anodes. Similarly, in proton exchange membrane (PEM) fuel cells the Nafion membrane as well as the ionomer phase in the catalyst layers swell with increase in water content, affecting cell resistance.[3] Mathematical models from the literature have considered volume changes in porous electrodes.[1,4-7] Many of these treatments include detailed electrochemistry and nonuniform structural changes (e.g., porosity changes). For example, Alkire et al.[4] developed a model for describing the nonuniform porosity changes occurring during anodic dissolution of a copper electrode. Assuming cylindrical pores, they analyzed the effects of porosity changes on the electrode resistance and reaction current distribution. Dunning et al.[5] developed a battery model to describe mass transfer of sparingly soluble active material, which was extended by them[6] to describe the operation of silver–silver chloride and cadmium–cadmium hydroxide electrodes. Using this model they treated the effects of changing porosity and reaction surface area in addition to charge and mass transport occurring in the electrodes. A more detailed review of these and other models considering structural changes in porous electrodes is given in Newman and Thomas-Alyea.[7] However, as pointed out by these latter authors,[7] all the models in the literature considering structural changes in porous electrodes assume a constant geometric volume for the electrode throughout its operation. Porosity is allowed to change during operation but expansion or contraction is either ignored or built into the initial conditions. For example, Jain et al.[1] treated cathode swelling in their Li–$SOCl_2$ battery model by using effective values for electrode thickness and initial porosity. This method assumes constant electrode thickness during discharge resulting in significant errors in the electrode resistance. Further, their method assumes uniform swelling at all points in the cathode, making it applicable only under conditions of near-uniform reaction distribution (e.g., low-rate discharges). In Li-ion batteries, Botte[8] and Christensen and Newman[9] modeled volume changes occurring in a single host particle but did not consider its effects on the volume changes of the porous electrode.

In this paper we present a three-dimensional mathematical model to describe volume changes occurring in porous electrodes. Based on material conservation equations we derive the governing equations relating the two effects of volume changes, namely, the change in the dimensions of the electrode and the change in its porosity. A parameter, called the swelling coefficient, is introduced so as to determine the relative magnitudes of the two effects. For a given electrochemical cell the swelling coefficient is obtained experimentally as discussed later. We consider three types of porous electrodes: (a) deposition/precipitation electrodes (e.g., the carbon cathode in Li/$SOCl_2$ batteries, which expands as LiCl is deposited in the pores), (b) intercalation electrodes (e.g., a Cu–Sn alloy anode in Li-ion batteries, which expands as Li intercalates), and (c) ionomer-based electrodes (e.g., the catalyst layer in PEM fuel cells, which expands as water content of its ionomer phase increases). The model is general and forms a critical addition required to extend the existing porous electrode models to include volume change effects. For the special case of uniform reaction distribution, analytical solutions are presented and used to illustrate the effect of volume changes in porous electrodes.

Model Development

Deposition/precipitation electrodes.— Figure 1 shows a schematic of a deposition/precipitation porous electrode. During operation, a solid-phase reaction product forms on the surface of the electrode particles, occupying a part of the pore volume and pushing the electrode particles away from each other. Thus, the volume change effects during operation manifest in two forms: (*i*) change in electrode dimensions and (*ii*) change in porosity. At all times, electronic connection is assumed to exist between the particles either through direct physical contact between them or through the electronically conductive binder interconnections. The relationship governing volume changes in the electrode is obtained from an overall material balance of the solid phase (electrode active material + reaction product + binder + filler + etc.) as

$$\frac{\partial}{\partial t}(1-\varepsilon) + \nabla \cdot [(1-\varepsilon)\mathbf{u}] = -\frac{s\hat{V}}{nF}j \qquad [1]$$

The local electrode velocity, $\mathbf{u}$, is a vector having the components of magnitudes, u_x, u_y, u_z in the x, y, z directions, respectively. Setting the normal velocities to zero at the planes, $x = 0$, $y = 0$, and $z = 0$ gives the boundary conditions

$$\text{at } w = 0,\ u_w = 0, \quad w = x,\ y,\ z \qquad [2]$$

This means that (*i*) the x velocity of the electrode–current collector interface is chosen as reference and set to zero and (*ii*) the y and z velocities of the center planes $y = 0$ and $z = 0$ are zero, a result of symmetry. The initial condition is set as

$$\text{at } t = 0,\ \varepsilon = \varepsilon^0 \qquad [3]$$

Expanding Eq. 1 and using Eq. 2, we get

* Electrochemical Society Student Member.
** Electrochemical Society Active Member.
[a] Present address: Medtronic Energy and Component Center, Brooklyn Center, Minnesota 55430, USA.
[z] E-mail: partha.m.gomadam@medtronic.com

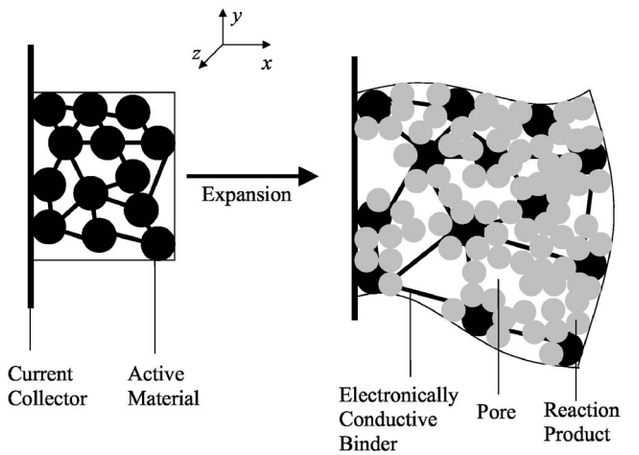

Figure 1. Schematic representation of a porous deposition/precipitation electrode before and after expansion. The electrode dimensions and porosity are functions of time and position. For illustrative purposes, the active material and the reaction product are shown regularly shaped. The electrode–current collector interface is set as $x = 0$. The center planes of the electrode in the y and z directions are set as $y = 0$ and $z = 0$, respectively.

$$\frac{1}{(1-\varepsilon)}\left[\frac{\partial}{\partial t}(1-\varepsilon) + \mathbf{u}\cdot\nabla(1-\varepsilon)\right] + \nabla\cdot\mathbf{u} = -\frac{s\hat{V}}{nF}\frac{j}{(1-\varepsilon)} \quad [4]$$

and

$$\text{at } w = 0,\ \frac{1}{(1-\varepsilon)}\left[\frac{\partial}{\partial t}(1-\varepsilon) + \sum_{\substack{v=x,y,z \\ v\neq w}} u_v\frac{\partial}{\partial v}(1-\varepsilon)\right] + \nabla\cdot\mathbf{u} = -\frac{s\hat{V}}{nF}\frac{j}{(1-\varepsilon)},\quad w = x,\ y,\ z \quad [5]$$

For a differential volume element, dV, in the electrode, Eq. 4 means that the rate of volume change due to product formation (the right side) is equal to the total rate of change of porosity (the bracketed term on the left side, which is equal to $d\ln(1-\varepsilon)/dt$) plus the rate of change of volume (the $\nabla\cdot\mathbf{u}$ term, which is equal to $d\ln dV/dt$). However, Eq. 4 and 5 are not sufficient to determine the magnitude of each of these terms. In other words, we have two unknowns, ε and $\mathbf{u}$, but only one governing equation, Eq. 4. Rigorously, a force balance equation is needed that relates the porosity and velocity to the physical and mechanical properties of the electrode and the cell. However, we resolve this problem empirically by introducing a swelling coefficient, g, such that Eq. 4 can be split into

$$\nabla\cdot\mathbf{u} = g\left[-\frac{s\hat{V}}{nF}\frac{j}{(1-\varepsilon)}\right] \quad [6]$$

and

$$\frac{\partial(1-\varepsilon)}{\partial t} + \mathbf{u}\cdot\nabla(1-\varepsilon) = (1-g)\left[-\frac{s\hat{V}}{nF}j\right] \quad [7]$$

and Eq. 5 into

$$\text{at } w = 0,\ \nabla\cdot\mathbf{u} = g\left[-\frac{s\hat{V}}{nF}\frac{j}{(1-\varepsilon)}\right],\quad w = x,\ y,\ z \quad [8]$$

and

$$\text{at } w = 0,\ \frac{1}{(1-\varepsilon)}\left[\frac{\partial}{\partial t}(1-\varepsilon) + \sum_{\substack{v=x,y,z \\ v\neq w}} u_v\frac{\partial}{\partial v}(1-\varepsilon)\right] = (1-g)\left[-\frac{s\hat{V}}{nF}j\right],\quad w = x,\ y,\ z \quad [9]$$

This means that a fraction, g, of the volume change due to product formation goes to change the electrode dimensions and the rest goes to change the porosity. For a given volume change due to product formation, we now have Eq. 3, 7, and 9, to solve for ε, and Eq. 2 and 6 to solve for $\mathbf{u}$.

For a differential volume element, dV, the swelling coefficient, g, is defined mathematically as

$$g \equiv \frac{\dfrac{d\ln dV}{d\ln(1-\varepsilon)}}{1 + \dfrac{d\ln dV}{d\ln(1-\varepsilon)}} \quad [10]$$

The swelling coefficient depends on the conditions in the electrode such as the arrangement of particles, the mechanical properties of the electrode components, the header space available for electrolyte, and the pressure experienced by either face of the electrode. While for a given electrode and cell setup these quantities may be constant, g is probably a function of electrode porosity. In an electrode dense with particles (i.e., when porosity is low), a greater fraction of volume change due to product formation would go to change the electrode dimensions (i.e., g is large). For an electrode with high porosity, greater room is available to accommodate the particles, resulting in a greater change in porosity (i.e., g is small). Regardless, the actual value or functional form of g for an electrode should be determined experimentally for a given electrode and cell design. The limits on g are 0 and 1; $g = 0$ means all the volume change due to product formation goes to change the electrode porosity with its dimensions remaining constant, and $g = 1$ means all the volume change due to product formation goes to change the dimensions of the electrode with its porosity remaining constant. As mentioned earlier, the limiting case of $g = 0$ is the more common assumption used in the literature to model volume change.[1,4-7]

The volume fraction of the electrode's active material, ε_e, is calculated from material balance as

$$\frac{\partial\varepsilon_e}{\partial t} + \nabla\cdot(\varepsilon_e\mathbf{u}) = 0 \quad [11]$$

with the initial condition

$$\text{at } t = 0,\ \varepsilon_e = \varepsilon_e^0 \quad [12]$$

and the boundary conditions

$$\text{at } w = 0,\ \frac{\partial\varepsilon_e}{\partial t} + \sum_{\substack{v=x,y,z \\ v\neq w}} u_v\frac{\partial\varepsilon_e}{\partial v} + \varepsilon_e\nabla\cdot\mathbf{u} = 0,\quad w = x,\ y,\ z \quad [13]$$

Unlike Eq. 1, Eq. 11 need not be split because $\mathbf{u}$ is calculated together with ε using Eq. 2 and 6 and Eq. 3, 7, and 9, respectively. The geometric volume of the electrode is calculated using the relation

$$\partial V/\partial t = \int_V (\nabla\cdot\mathbf{u})dV \quad [14]$$

and the initial condition

$$\text{at } t = 0,\ V = V^0 \quad [15]$$

If expansion occurs equally in all directions, then the changes in the dimensions of the electrode is given by the cube root of the change

in electrode volume. However, when expansion occurs differently in different directions, we need to calculate the individual components of the velocity to calculate the dimensions of the electrode. In other words, rewriting Eq. 6 in terms of the component velocities as

$$\frac{\partial u_x}{\partial x} + \frac{\partial u_y}{\partial y} + \frac{\partial u_z}{\partial z} = g\left[-\frac{s\hat{V}}{nF}\frac{j}{(1-\varepsilon)}\right] \quad [16]$$

shows that we have three unknowns, u_x, u_y, u_z, and only one governing equation, Eq. 16. To obtain the component velocities we introduce further splitting parameters, g_x, g_y, g_z, such that Eq. 16 can be split into

$$\frac{\partial u_x}{\partial x} = g_x g\left[-\frac{s\hat{V}}{nF}\frac{j}{(1-\varepsilon)}\right] \quad [17]$$

$$\frac{\partial u_y}{\partial y} = g_y g\left[-\frac{s\hat{V}}{nF}\frac{j}{(1-\varepsilon)}\right] \quad [18]$$

$$\frac{\partial u_z}{\partial z} = g_z g\left[-\frac{s\hat{V}}{nF}\frac{j}{(1-\varepsilon)}\right] \quad [19]$$

The parameters, g_x, g_y, and g_z, determine how much of the electrode's geometric volume change occurs due to change in its dimensions in the x, y, and z directions, respectively. Mathematically, they are defined as

$$g_x \equiv \frac{d\ln dx}{d\ln dV} \quad [20]$$

$$g_y \equiv \frac{d\ln dy}{d\ln dV} \quad [21]$$

$$g_z \equiv \frac{d\ln dz}{d\ln dV} \quad [22]$$

Thus, we now have three governing equations (i.e., Eq. 17-19) and the boundary conditions (i.e., Eq. 2) to solve for the three component velocities, u_x, u_y, u_z. The corresponding electrode dimensions, $L_x(y,z)$, $L_y(z,x)$, $L_z(x,y)$, are obtained as functions of time from the equations

$$\frac{dL_x}{dt} = u_x\big|_{x=L_x} \quad [23]$$

$$\frac{dL_y}{dt} = u_y\big|_{y=L_y} \quad [24]$$

$$\frac{dL_z}{dt} = u_z\big|_{z=L_z} \quad [25]$$

with the initial conditions that

$$\text{at } t = 0,\ L_x = L_x^0,\ L_y = L_y^0,\ L_z = L_z^0 \quad [26]$$

In the above equations we have introduced four parameters, namely, g, g_x, g_y, and g_z. However, adding Eq. 17-19 and comparing with Eq. 16 gives

$$g_x + g_y + g_z = 1 \quad [27]$$

Further, in most electrodes the changes in dimensions would occur equally in the y and z directions, giving

$$g_y = g_z = \frac{1-g_x}{2} \quad [28]$$

Thus, in most situations the required number of parameters is reduced to two: g and g_x.

The special case of uniform reaction current.— The model presented above is rigorous and applicable for all deposition/precipitation porous electrodes. However, for illustrative purposes we consider the special case of an electrode with a uniform initial porosity and a uniform reaction current, giving

$$j = \frac{I}{V} \quad [29]$$

and

$$\nabla(1-\varepsilon) = 0 \quad [30]$$

where I is the total current in amperes applied to or supplied by the electrode. Therefore, j, ε, and the electrode dimensions, L_x, L_y, L_z, are functions of time only. Further, Eq. 30 means that the second terms on the left sides of Eq. 7 and 9 become zero, and therefore, they can be solved independently of **u**. Finally, for a constant g and for galvanostatic operation (i.e., for I = constant), Eq. 2, 3, 6, 7, 9, and 14 are solved analytically to obtain

$$\frac{1-\varepsilon}{1-\varepsilon^0} = \left[1 + \left(\frac{\varepsilon^0}{1-\varepsilon^0}\right)\frac{t}{\tau^0}\right]^{1-g} \quad [31]$$

$$\frac{\varepsilon_e}{\varepsilon_e^0} = \left[1 + \left(\frac{\varepsilon^0}{1-\varepsilon^0}\right)\frac{t}{\tau^0}\right]^{-g} \quad [32]$$

and

$$\frac{V}{V^0} = \left[1 + \left(\frac{\varepsilon^0}{1-\varepsilon^0}\right)\frac{t}{\tau^0}\right]^{g} \quad [33]$$

In Eq. 31-33, τ^0 is a characteristic operating time of the electrode defined as

$$\tau^0 \equiv \frac{\varepsilon^0 V^0}{\left(-\frac{s\hat{V}}{nF}I\right)} \quad [34]$$

which is the ratio of the initial pore volume to the rate of pore filling. Thus, τ^0 gives the galvanostatic operating time (i.e., the time taken to fill the pores completely) for the case when there is no change in the geometric volume of the electrode (i.e., when $g = 0$). When both the electrode porosity and geometric volume change (i.e., when $g \neq 0$), the operating time, τ, is calculated from Eq. 31 by setting ε to zero. Thus

$$\frac{\tau}{\tau^0} = \frac{(1-\varepsilon^0)^{-g/1-g} - (1-\varepsilon^0)}{\varepsilon^0} \quad [35]$$

The dimensions of the electrode are obtained by solving Eq. 2 and 17-26 as

$$\frac{L_x}{L_x^0} = \left[1 + \left(\frac{\varepsilon^0}{1-\varepsilon^0}\right)\frac{t}{\tau^0}\right]^{g_x g} \quad [36]$$

$$\frac{L_y}{L_y^0} = \left[1 + \left(\frac{\varepsilon^0}{1-\varepsilon^0}\right)\frac{t}{\tau^0}\right]^{g_y g} \quad [37]$$

$$\frac{L_z}{L_z^0} = \left[1 + \left(\frac{\varepsilon^0}{1-\varepsilon^0}\right)\frac{t}{\tau^0}\right]^{g_z g} \quad [38]$$

and

$$\frac{A}{A^0} = \left[1 + \left(\frac{\varepsilon^0}{1-\varepsilon^0}\right)\frac{t}{\tau^0}\right]^{(g_y+g_z)g} = \left[1 + \left(\frac{\varepsilon^0}{1-\varepsilon^0}\right)\frac{t}{\tau^0}\right]^{(1-g_x)g} \quad [39]$$

The changes in the ionic and electronic resistances of the electrode due to volume change during operation are given by

$$\frac{R_i}{R_i^0} = \frac{(L_x/L_x^0)}{(A/A^0)(\varepsilon/\varepsilon^0)^{1.5}} \quad [40]$$

and

$$\frac{R_e}{R_e^0} = \frac{(L_x/L_x^0)}{(A/A^0)(\varepsilon_e/\varepsilon_e^0)^{1.5}} \quad [41]$$

where the ionic and electronic conductivities are assumed to be proportional to $\varepsilon^{1.5}$ and $\varepsilon_e^{1.5}$, respectively.[7] The kinetic resistance of the electrode remains a constant because it is a function of the quantity, aV, which is proportional to the constant quantity, $\varepsilon_e V$ (see Eq. 32 and 33).

Intercalation electrodes.— In an intercalation electrode, volume changes occur in the solid phase when the product of electrochemical reaction intercalates into the active material particles of the electrode. As the particles expand during intercalation, they occupy a greater part of the pore volume and at the same time push each other away. If the volume change of mixing is negligible, the same equations as for deposition/precipitation electrodes are applicable. When volume change in mixing is significant, the governing relationship between porosity and electrode dimensions is derived by observing that the number of particles in the electrodes is conserved as the electrode volume changes. Thus

$$\frac{\partial}{\partial t}\left(\frac{1-\varepsilon}{V_p}\right) + \nabla \cdot \left(\frac{1-\varepsilon}{V_p}\mathbf{u}\right) = 0 \quad [42]$$

where V_p is the volume of an electrode particle and $(1-\varepsilon)/V_p$ is the number of particles per unit volume of the electrode. Expanding Eq. 42 we get

$$\frac{1}{(1-\varepsilon)}\left[\frac{\partial}{\partial t}(1-\varepsilon) + \mathbf{u}\cdot\nabla(1-\varepsilon)\right] + \nabla\cdot\mathbf{u} = \frac{1}{V_p}\left(\frac{\partial V_p}{\partial t} + \mathbf{u}\cdot\nabla V_p\right) \quad [43]$$

which means that the volume change in the electrode particles due to intercalation (the right side) translates into the combined effect of the change in porosity (the bracketed term on the left side) and the change in electrode dimensions (the $\nabla\cdot\mathbf{u}$ term). If volume change in mixing is negligible, then the change in particle volume is proportional to the local reaction rate. Therefore, Eq. 43 reduces to Eq. 4 with $\hat{V}$ representing the molar volume of pure intercalate. When volume change in mixing is significant, Eq. 43 should be used, wherein the particle volume is obtained from material balance of the intercalation process occurring inside the particle. The rest of the analysis is the same as for deposition/precipitation electrodes except that here $\varepsilon_e = 1-\varepsilon$. For the special case of uniform reaction distribution under galvanostatic discharge, the porosity and electrode volume are solved analytically as

$$\frac{1-\varepsilon}{1-\varepsilon^0} = \left(\frac{V_p}{V_p^0}\right)^{(1-g)} \quad [44]$$

$$\frac{V}{V^0} = \left(\frac{V_p}{V_p^0}\right)^{g} \quad [45]$$

$$\frac{L_x}{L_x^0} = \left(\frac{V_p}{V_p^0}\right)^{g_x g} \quad [46]$$

$$\frac{L_y}{L_y^0} = \left(\frac{V_p}{V_p^0}\right)^{g_y g} \quad [47]$$

$$\frac{L_z}{L_z^0} = \left(\frac{V_p}{V_p^0}\right)^{g_z g} \quad [48]$$

and

$$\frac{A}{A^0} = \left(\frac{V_p}{V_p^0}\right)^{(g_y+g_z)g} = \left(\frac{V_p}{V_p^0}\right)^{(1-g_x)g} \quad [49]$$

Note that in contrast to deposition/precipitation electrodes, the time of operation for an intercalation electrode is independent of pore volume and therefore, is independent of the swelling coefficient.

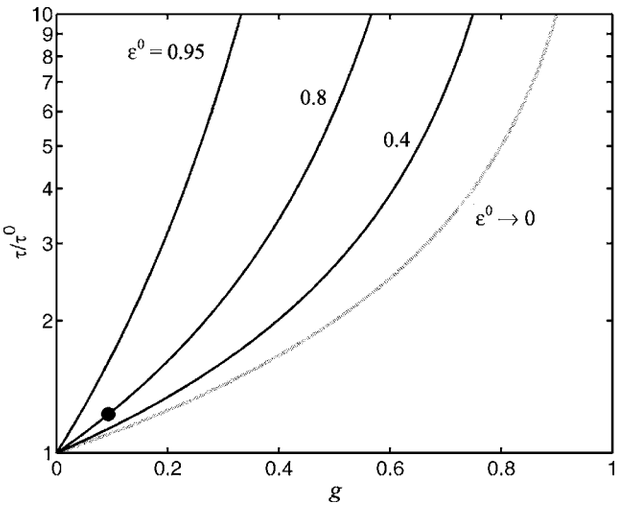

Figure 2. A plot of Eq. 35 showing the effect of g and the initial porosity, ε^0, on the operating time, τ. The gray line is $\tau/\tau^0 = 1/(1-g)$, which is the limit as $\varepsilon^0 \to 0$. As $\varepsilon \to 1$, τ/τ^0 approaches the y axis. The point marked ● shows that for the case of Jain et al.,[1] where $\tau/\tau^0 = 1.267$ and $\tau^0 = 0.8$, $g = 0.107$.

Ionomer-based electrodes.— In an ionomer-based electrode such as a carbon–ionomer fuel cell catalyst, volume changes occur in the ionomer phase when it absorbs water. As the ionomer volume increases, it occupies a greater volume fraction in the electrode and at the same time pushes the active material particles away from each other. Applying a material balance over the ionomer phase gives the governing relationship between the volume fraction of the ionomer phase, ε_i, and the local velocity of the electrode as

$$\frac{\partial}{\partial t}(\varepsilon_i c_i) + \nabla\cdot(\varepsilon_i c_i \mathbf{u}) = 0 \quad [50]$$

On expanding, Eq. 50 becomes

$$\frac{1}{\varepsilon_i}\left(\frac{\partial \varepsilon_i}{\partial t} + \mathbf{u}\cdot\nabla\varepsilon_i\right) + \nabla\cdot\mathbf{u} = -\frac{1}{c_i}\left(\frac{\partial c_i}{\partial t} + \mathbf{u}\cdot\nabla c_i\right) \quad [51]$$

which is of the same form as Eq. 4 or 43. The right side of Eq. 51 gives the volume change in the ionomer phase, where the ionomer concentration, c_i, is obtained from a material balance over the absorbed species. Following the same analysis as for deposition/precipitation electrodes, ε_i is obtained by solving Eq. 51 along with the initial condition that

$$\text{at } t = 0,\ \varepsilon_i = \varepsilon_i^0 \quad [52]$$

The porosity of the electrode is calculated by noting that $\varepsilon = 1 - \varepsilon_i - \varepsilon_e$.

Results and Discussion

For a given reaction rate distribution, $j(x,y,z,t)$, the model presented here can be used to calculate the porosity and electrode dimensions as functions of time and position in the electrode. To calculate the reaction rate distribution, the model should be solved simultaneously with charge balances in the ionic and electronic phases and material balances for the various species involved. However, for illustrative purposes, here we analyze the effect of volume changes in a deposition/precipitation electrode under conditions of uniform current distribution when the analytical solutions given in Eq. 31-41 apply.

The dimensionless operating time, τ/τ^0, given by Eq. 35, is a function of two parameters, g and ε^0, and independent of g_x. In Fig. 2, Eq. 35 is used to plot τ/τ^0 vs g for various initial porosities,

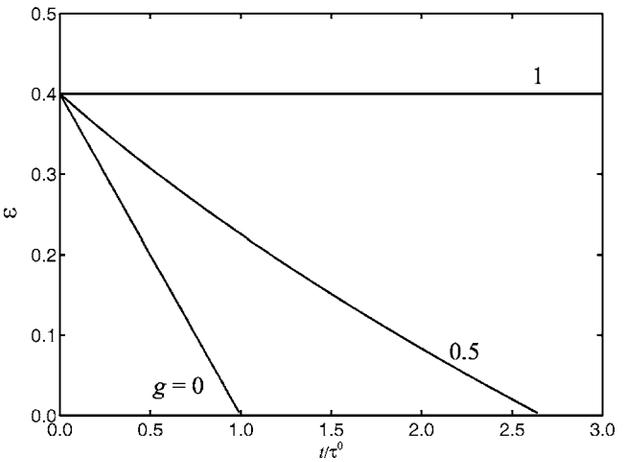

Figure 3. A plot of Eq. 31 showing the effect of the swelling coefficient, g, on the electrode porosity during operation. The initial porosity, ε^0, is 0.4. The electrode porosity is independent of the value of g_x.

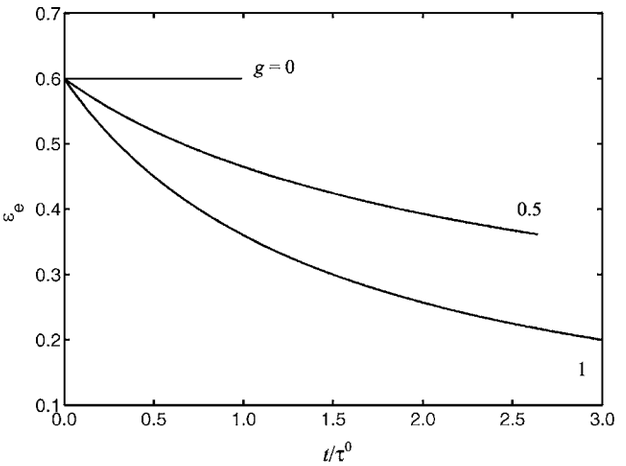

Figure 4. A plot of Eq. 32 showing the effect of the swelling coefficient, g, on the volume fraction of the electrode's active material during operation. The initial porosity, ε^0, is 0.4. The active material volume fraction is independent of the value of g_x.

ε^0. By definition, $\tau/\tau^0 = 1$ when $g = 0$, i.e., the operating time approaches the characteristic operating time, τ^0, when there is no change in the geometric volume of the electrode. As g increases, the operating time increases, approaching infinity as $g \rightarrow 1$. In this limit, the geometric volume change of the electrode is unconstrained and discharge continues indefinitely. That is, the volume of the electrode continues to increase to accommodate the product formed while the porosity remains constant. For a given g, the dimensionless operating time, τ/τ^0, decreases with decrease in the initial porosity, approaching the limit $1/(1 - g)$ as the initial porosity approaches zero. The actual discharge time also decreases with decrease in initial porosity approaching zero as the initial porosity approaches zero. When the initial porosity is high (i.e., as $\varepsilon^0 \rightarrow 1$) the operating time approaches infinity even for small values of g. The point marked ● shows that for the case of Jain et al.,[1] where $\tau/\tau^0 = 1.267$ and $\varepsilon^0 = 0.8$, $g = 0.107$. Most practical battery systems would probably reside in the lower left region of Fig. 2. Even in these practical cases, though, the volume change effects are significant.

The swelling coefficient, g, is not an intrinsic property of an electrode but rather a design-dependent one. An expanding electrode can be designed to have a higher g value by using, for example, a more elastic binder or by providing extra space for expansion. For deposition/precipitation electrodes, the actual value of g is obtained for each design using discharge data and cell parameters in conjunction with Fig. 2 or Eq. 35. For example, Jain et al.[1] observed a low-rate discharge capacity of 16.7 Ah. Based on the initial thickness (0.07 cm) and initial porosity (0.8) measured prior to cell assembly, a capacity of 13.18 Ah was estimated by Jain et al.,[1] assuming that no swelling occurred (i.e., $g = 0$). Therefore, $\tau/\tau^0 = 16.7/13.18 = 1.267$. Using this value for τ/τ^0 and with $\varepsilon^0 = 0.8$, a value for $g = 0.107$ is obtained from Fig. 2 (or Eq. 35).

The evolution of porosities, ε and ε_e, with time are functions of g and ε^0 only, as seen from Eq. 31 and 32. In Fig. 3 and 4, these equations are plotted for various values of g, keeping $\varepsilon^0 = 0.4$. Figure 3 shows that when $g \neq 1$, the porosity decreases with time and reaches zero when $t/\tau^0 = \tau/\tau^0$. For $\varepsilon^0 = 0.4$, Fig. 2 gives the dimensionless operating times as $\tau/\tau^0 = 1$, 2.66, and ∞ for $g = 0$, 0.5, and 1, respectively. When $g = 1$, the porosity remains constant and, therefore, the operating time is infinitely large. Figure 4 shows the change in the volume fraction of the electrode active material, ε_e, during operation. When $g \neq 0$ the geometric volume of the electrode increases causing ε_e to decrease with time because $\varepsilon_e V$ = constant. When $g = 0$, the geometric volume remains constant and therefore, ε_e also remains constant. The porosity, ε, the active material volume fraction, ε_e, and the geometric volume of the electrode, V, are independent of g_x, as seen from Eq. 31-33.

The evolution of L_x, A, R_i, and R_e with time are functions of g, ε^0, as well as g_x, as seen from Eq. 36 and 39-41. In Fig. 5-8, these equations are plotted as functions of time for $\varepsilon^0 = 0.4$ and for various combinations of g and g_x. In the figures, the black lines are plotted for various values of g, keeping $g_x = 1/3$, while the gray lines are plotted for various values of g_x, keeping $g = 0.5$. For the case of no volume change (i.e., $g = 0$), both the electrode thickness, L_x, and cross-sectional area, A, remain constant at their initial values. When $g \neq 0$, both thickness and area change with time, with area increasing faster than thickness when $g_x = 1/3$, as shown by the black lines. For a given g, the electrode thickness and area change with time such that their product (i.e., the electrode volume, V) remains the same for all values of g_x. However, with increase in g_x, volume change in the electrode occurs more through thickness change and less through area change. In the limit when $g_x = 0$, thickness remains constant and all the volume change occurs

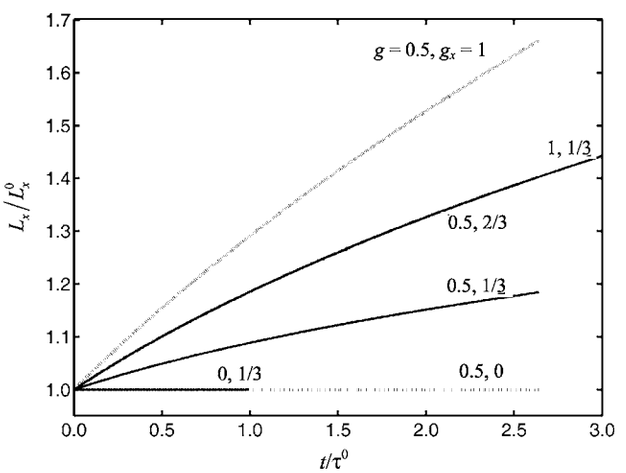

Figure 5. A plot of Eq. 36 showing the effect of the parameters, g and g_x, on the electrode thickness during operation. The initial porosity, ε^0, is 0.4. The black lines are plotted for various values of g, keeping $g_x = 1/3$. The gray lines are plotted for various values of g_x, keeping $g = 0.5$.

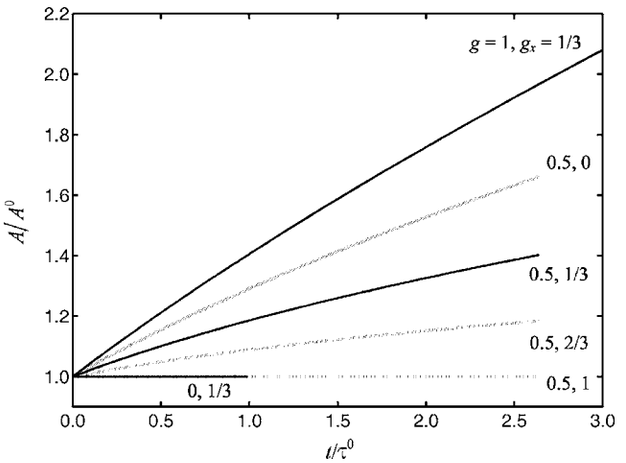

Figure 6. A plot of Eq. 39 showing the effect of the parameters, g and g_x, on the electrode area during operation. The initial porosity, ε^0, is 0.4. The black lines are plotted for various values of g, keeping $g_x = 1/3$. The gray lines are plotted for various values of g_x, keeping $g = 0.5$.

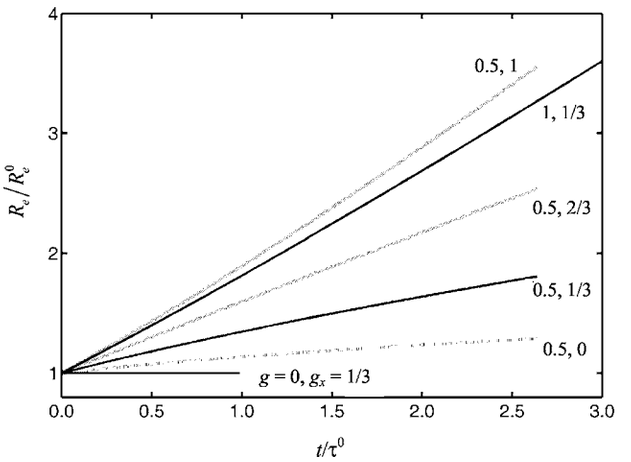

Figure 8. A plot of Eq. 41 showing the effect of the parameters, g and g_x, on the electronic resistance of the electrode during operation. The initial porosity, ε^0, is 0.4. The black lines are plotted for various values of g, keeping $g_x = 1/3$. The gray lines are plotted for various values of g_x, keeping $g = 0.5$.

through area change. Conversely, when $g_x = 1$, area remains constant and all the volume change occurs through thickness change. Note that from Eq. 36 the electrode length depends only on the product of g and g_x, causing the black lines ($g_x = 1/3$) and gray lines ($g = 0.5$) to overlap when the product is the same. Similarly, from Eq. 39 the electrode area depends only on the product of g and $(1 - g_x)$, causing the black and gray lines to overlap when their product is the same.

Figure 7 and 8 show the effect of volume changes on the ionic and electronic resistances, R_i and R_e, of the electrode. As before, the black lines are plotted for various values of g, keeping $g_x = 1/3$, while the gray lines are plotted for various values of g_x, keeping $g = 0.5$. For $g = 0$ or 0.5, porosity decreases and, consequently, ionic resistance increases, while for $g = 1$ the ionic resistance decreases even though the porosity remains constant. This is because the resistance depends also on the ratio, L_x/A, which decreases because area increases faster than thickness when $g_x = 1/3$. In contrast, ε_e decreases faster than L_x/A, resulting in an increase in the electronic resistance when $g \neq 0$. When $g = 0$, ε_e, L_x, and A remain constant, therefore, the electronic resistance also remains constant. Finally, the ionic and electronic resistances of the electrode increase with g_x because L_x/A increases with g_x, as seen from Eq. 36 and 39. Note that if the ionic and electronic resistances are equally important at the beginning of operation, then the electrode becomes ionically limited for small values of g and electronically limited for large values of g. Further, the end of operation is generally determined by a cutoff voltage, which depends on the resistances in the electrode. For example, in the case of a $LiSOCl_2$ battery cathode of Jain et al.,[1] a drop in the electrode voltage of 1.5 V from its initial value is taken to be end of discharge. Assuming that the electrode is ionically limited, this means that for the low-rate discharge, where the initial voltage drop is 0.3 V, discharge ends when $R_i/R_i^0 = 5$. For $g = 0$ or 0.5, we see that this occurs well before the pores are completely filled.

In contrast to the ionic and electronic resistances, the kinetic resistance of the electrode remains a constant (not shown) for all values of g and g_x if the specific surface area of the electrode varies linearly with the volume fraction of the electrode's active material.

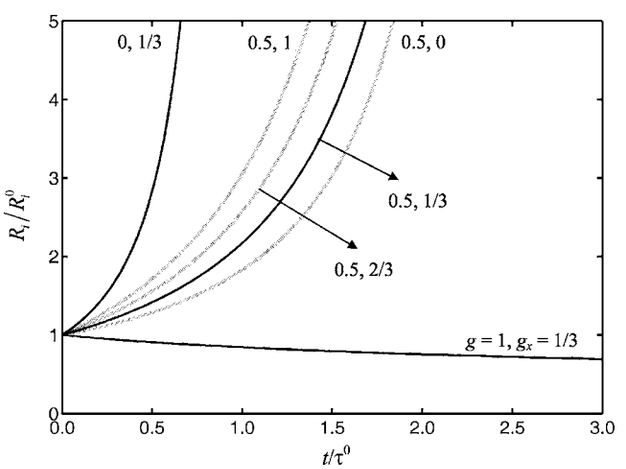

Figure 7. A plot of Eq. 40 showing the effect of the parameters, g and g_x, on the ionic resistance of the electrode during operation. The initial porosity, ε^0, is 0.4. The black lines are plotted for various values of g, keeping $g_x = 1/3$. The gray lines are plotted for various values of g_x, keeping $g = 0.5$.

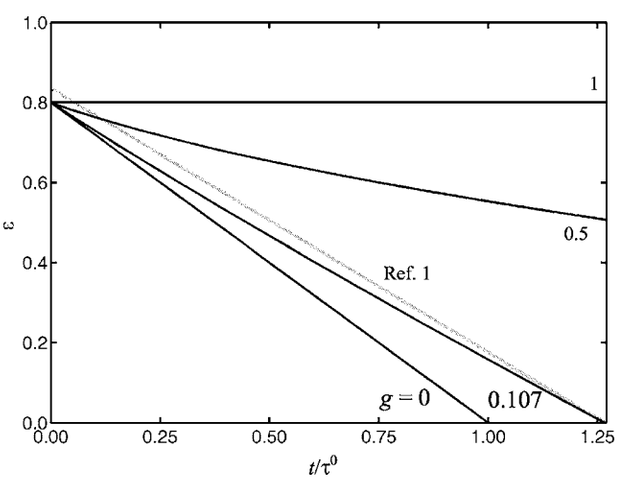

Figure 9. A plot of Eq. 31 showing the effect of g on porosity during operation, when $\varepsilon^0 = 0.8$ and $g_x = 1$. The gray line shows the method of Jain et al.[1]

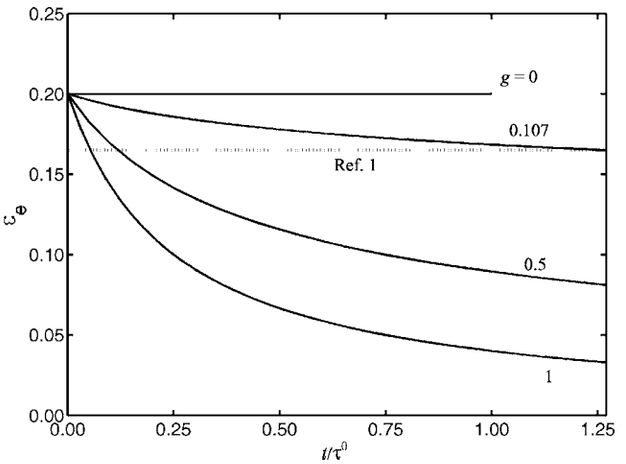

Figure 10. A plot of Eq. 32 showing the effect of g on volume fraction of the electrode's active material during operation, when $\varepsilon^0 = 0.8$ and $g_x = 1$. The gray line shows the method of Jain et al.[1]

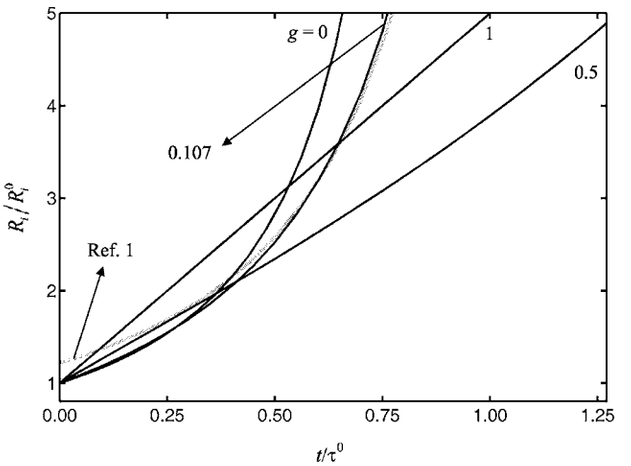

Figure 12. A plot of Eq. 40 showing the effect of g on the ionic resistance of the electrode during operation, when $\varepsilon^0 = 0.8$ and $g_x = 1$. The gray line shows the method of Jain et al.[1]

As mentioned in the Model Development section, the kinetic resistance depends on the product $\varepsilon_e V$, which is a constant.

As mentioned earlier, g can be obtained by using the experimentally observed operating time in Eq. 35. Similarly, g_x can be obtained experimentally from Eq. 36 and the knowledge of the change of electrode thickness during operation. Alternatively, g_x can be estimated by fitting Eq. 40 and 41 to measured resistance during operation.

Figures 9-13 show the effect of volume changes in the electrode for the case when $\varepsilon^0 = 0.8$ and $g_x = 1$ (i.e., constant cross-sectional area). The black lines are plotted for $g = 0$, 0.107, 0.5, and 1, while the gray lines are based on the approach of Jain et al.[1] They accounted for swelling by using higher values for electrode thickness (0.085 cm) and initial porosity (0.835) than what was measured prior to cell assembly so as to match the observed capacity (i.e., 16.7 Ah). The case of $g = 0.107$ corresponds to the $LiSOCl_2$ battery cathode of Jain et al.,[1] marked ● in Fig. 2. While the porosity change with time predicted by Jain et al.[1] lies close to ours (Fig. 9), the electrode thickness (Fig. 10) and active material volume fraction (Fig. 11) are qualitatively different. This results in a maximum error of 25% in the ionic and electronic resistances (Fig. 12 and 13) and, consequently, on the electrode voltage. For example, for the moderate-rate discharge considered by Jain et al.,[1] the initial voltage drop is 0.6 V, which means a maximum error of 0.15 V when using their method. At higher rates, this error would proportionally increase because the initial voltage drop directly scales with the discharge rate. Further, larger errors in the predicted voltages would occur for higher values of g because the electrode thickness and active material volume fraction change more.

The effect of increasing g on the electrode porosity, active material volume fraction, and length are qualitatively the same as observed earlier in Fig. 3-6. However, because $g_x = 1$ the electrode thickness increases faster, resulting in the ionic and electronic resistances reaching cutoff values much sooner than porosity becoming zero. In contrast to Fig. 7 and 8, the operating times based on cutoff voltage in Fig. 12 and 13 decrease with increase in g if electronically limited, or increase first and then decrease with increase in g if ionically limited.

Conclusion

A mathematical model was developed to describe volume changes in three dimensions occurring in (*i*) deposition/precipitation, (*ii*) intercalation; and (*iii*) ionomer-based porous elec-

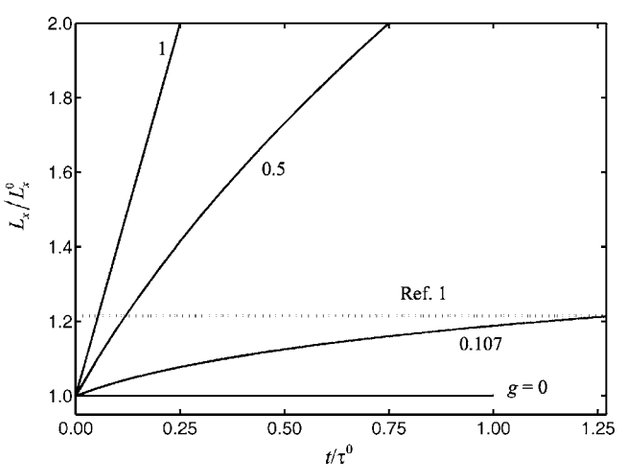

Figure 11. A plot of Eq. 36 showing the effect of g on electrode thickness during operation, when $\varepsilon^0 = 0.8$ and $g_x = 1$. The gray line shows the method of Jain et al.[1]

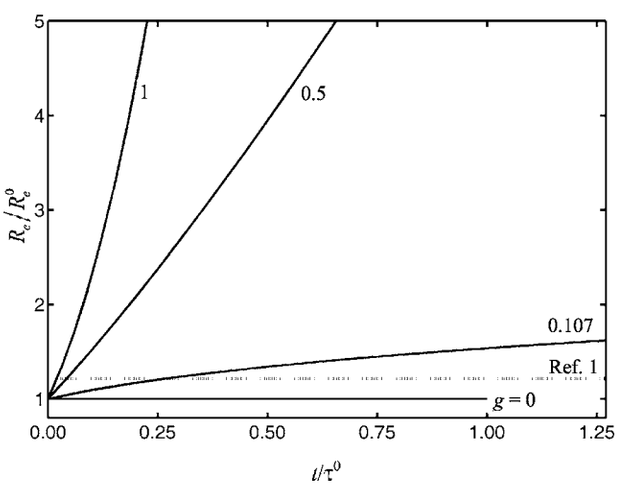

Figure 13. A plot of Eq. 41 showing the effect of g on the electronic resistance of the electrode during operation, when $\varepsilon^0 = 0.8$ and $g_x = 1$. The gray line shows the method of Jain et al.[1]

trodes. The effects of volume changes on the electrode are identified to be twofold, namely, change in electrode dimensions and change in porosity. Based on material conservation the governing relationship between porosity and electrode dimensions is derived. Key design-dependent parameters, g and g_x, are introduced, which determine the individual magnitudes of the changes in porosity and electrode dimensions. These parameters should be obtained experimentally for a given cell design as discussed.

For a given reaction rate, the models presented here allow calculation of porosity and electrode dimensions as functions of time and position in the electrode. To calculate the reaction rate distribution the model should be solved simultaneously with charge balances in the ionic and electronic phases and material balances for the various species involved. For the special case of galvanostatic operation with a uniform current distribution, analytical solutions are presented and used to illustrate the effect of volume changes. It is shown that the time of pore filling increases steeply with increase in g, which, in the case of a battery, means that electrode swelling results in greater discharge capacity. However, the operation time based on cutoff values of the resistances in the electrode increase or decrease with g depending on the value of g_x. The sensitivity of the operating time and the ionic and electronic resistances to these parameters demonstrates the importance of including volume change effects in porous electrode models. The models presented in this work are general and form critical additions required to extend the existing porous electrode models to include volume change effects.

The University of South Carolina assisted in meeting the publication costs of this article.

List of Symbols

a	specific surface area of porous electrode, cm^2/cm^3
A	cross-sectional area of porous electrode, cm^2
c_i	concentration of ionomer in ionomer phase, mol/cm^3
F	Faraday's constant, 96,487 C/mol
g	swelling coefficient introduced in Eq. 6 and 7
g_x, g_y, g_z	splitting parameters introduced in Eq. 17-19
I	total applied current, A
j	local volumetric electrochemical reaction rate, A/cm^3
L_x, L_y, L_z	dimensions of electrode in x, y, z directions, cm
n	number of electron transfers in electrochemical reaction
R_e	electronic resistance of porous electrode, Ω
R_i	ionic resistance of porous electrode, Ω
s	stoichiometric coefficient of the product in electrochemical reaction
t	time, s
$\mathbf{u}$	local velocity vector in the electrode, cm/s
u_x, u_y, u_z	magnitudes of the components of $\mathbf{u}$ in the x, y, z directions, cm/s
v	defined when used
V	total electrode volume, cm^3
$\hat{V}$	molar volume of reaction product, cm^3/mol
V_p	volume of intercalation particle, cm^3
w	defined when used
x, y, z	position in the electrode, cm

Greek

ε	porosity
ε_e	volume fraction of electrode active material
ε_i	volume fraction of ionomer phase
τ	operating time or time taken to fill pores completely, s
τ^0	operating time or time taken to fill pores completely when $g = 0$, s

Superscript

0	initial

References

1. M. Jain, G. Nagasubramanian, R. G. Jungst, and J. W. Weidner, *J. Electrochem. Soc.*, **146**, 4023 (1999).
2. J. Yang, Y. Takeda, Q. Li, N. Imanishi, and O. Yamamoto, *J. Power Sources*, **90**, 64 (2000).
3. P. Choi, N. H. Dalani, and R. Datta, *J. Electrochem. Soc.*, **152**, E123 (2005).
4. R. C. Alkire, E. A. Grens II, and C. W. Tobias, *J. Electrochem. Soc.*, **116**, 1328 (1969).
5. J. S. Dunning, D. N. Bennion, and J. Newman, *J. Electrochem. Soc.*, **118**, 1251 (1971).
6. J. S. Dunning, D. N. Bennion, and J. Newman, *J. Electrochem. Soc.*, **120**, 906 (1973).
7. J. Newman and K. E. Thomas-Alyea, *Electrochemical Systems*, 3rd ed., pp. 536–537, 523, John Wiley & Sons, New York (2004).
8. G. G. Botte, Abstract 314, The Electrochemical Society Meeting Abstracts, Vol. 2003-2 Orlando, FL, Oct 12–16, 2003.
9. J. Christensen and J. Newman, Abstract 611, The Electrochemical Society and the Electrochemical Society of Japan Meeting Abstracts, Vol. 2004-2 Honolulu, HI, Oct 3–8, 2004.